

Articles

Synthesis, pH-Dependent Structural Characterization, and Solution Behavior of Aqueous Aluminum and Gallium Citrate Complexes

M. Matzapetakis,[†] M. Kourgiantakis,[†] M. Dakanali,[†] C. P. Raptopoulou,[‡] A. Terzis,[‡] A. Lakatos,[§] T. Kiss,^{*,§} I. Banyai,^{||} L. Iordanidis,[⊥] T. Mavromoustakos,[⊗] and A. Salifoglou^{*,†}

Department of Chemistry, University of Crete, Heraklion 71409, Greece, Institute of Materials Science, NRCPS "Demokritos", Aghia Paraskevi 15310, Attiki, Greece, Department of Inorganic and Analytical Chemistry, University of Szeged, Szeged, H-6720 Hungary, Department of Physical Chemistry, Kossuth University, Debrecen, H-6720 Hungary, Department of Chemistry, Michigan State University, East Lansing, Michigan 48824-1322, and National Hellenic Research Foundation, Institute of Organic and Pharmaceutical Chemistry, Athens 11635, Greece

Received April 27, 2000

Reactions of Al(III) and Ga(III) with citric acid in aqueous solutions, yielded the complexes $(\text{NH}_4)_5\{\text{M}(\text{C}_6\text{H}_4\text{O}_7)_2\} \cdot 2\text{H}_2\text{O}$ (M(III) = Al (**1**), Ga (**2**)) at alkaline pH, and the complexes $(\text{Cat})_4\{\text{M}(\text{C}_6\text{H}_5\text{O}_7)(\text{C}_6\text{H}_4\text{O}_7)\} \cdot n\text{H}_2\text{O}$ (M(III) = Al (**3**), Ga (**4**), Cat. = NH_4^+ , $n = 3$; M(III) = Al (**5**), Ga (**6**), Cat. = K^+ , $n = 4$) at acidic pH. All compounds were characterized by spectroscopic (FT-IR, ^1H , ^{13}C , and ^{27}Al NMR, ^{13}C -MAS NMR) and X-ray techniques. Complex **1** crystallizes in space group $P\bar{1}$, with $a = 9.638(5)$ Å, $b = 9.715(5)$ Å, $c = 7.237(4)$ Å, $\alpha = 90.96(1)^\circ$, $\beta = 105.72(1)^\circ$, $\gamma = 119.74(1)^\circ$, $V = 557.1(3)$ Å³, and $Z = 1$. Complex **2** crystallizes in space group $P\bar{1}$, with $a = 9.659(6)$ Å, $b = 9.762(7)$ Å, $c = 7.258(5)$ Å, $\alpha = 90.95(2)^\circ$, $\beta = 105.86(2)^\circ$, $\gamma = 119.28(1)^\circ$, $V = 564.9(7)$ Å³, and $Z = 1$. Complex **3** crystallizes in space group $I2/a$, with $a = 19.347(3)$ Å, $b = 9.857(1)$ Å, $c = 23.412(4)$ Å, $\beta = 100.549(5)^\circ$, $V = 4389(1)$ Å³, and $Z = 8$. Complex **4** crystallizes in space group $I2/a$, with $a = 19.275(1)$ Å, $b = 9.9697(6)$ Å, $c = 23.476(1)$ Å, $\beta = 100.694(2)^\circ$, $V = 4432.8(5)$ Å³, and $Z = 8$. Complex **5** crystallizes in space group $P\bar{1}$, with $a = 7.316(1)$ Å, $b = 9.454(2)$ Å, $c = 9.569(2)$ Å, $\alpha = 64.218(4)^\circ$, $\beta = 69.872(3)^\circ$, $\gamma = 69.985(4)^\circ$, $V = 544.9(2)$ Å³, and $Z = 1$. Complex **6** crystallizes in space group $P\bar{1}$, with $a = 7.3242(2)$ Å, $b = 9.4363(5)$ Å, $c = 9.6435(5)$ Å, $\alpha = 63.751(2)^\circ$, $\beta = 70.091(2)^\circ$, $\gamma = 69.941(2)^\circ$, $V = 547.22(4)$ Å³, and $Z = 1$. The crystal structures of **1–6** reveal mononuclear octahedral complexes of Al(III) (or Ga(III)) bound to two citrates. Solution NMR, on both 4- and 5- species, reveals rapid intramolecular exchange of the bound and unbound terminal carboxylates. Upon dissolution in water, the complexes, through a complicated reaction cascade, transform to oligonuclear 1:1 species that, in agreement with previous studies, represent the thermodynamically stable state in solution. The data provide, for the first time, structural details of low MW, mononuclear complexes of Al(III) (or Ga(III)) with citrate that are dictated, among other factors, by pH. The properties of **1–6** may provide clues relevant to their biological association with humans.

Introduction

The involvement of aluminum and gallium in biological systems has been widely addressed in recent years.^{1,2} Their association with biological tissues emerges predominantly through their potential to interact with cellular components^{3,4} and to render their host cells largely differentiated from their native physiological state. Aluminum's biotoxic⁵ manifestations

have been linked, albeit not definitively, with Alzheimer's disease plaque and neurofibrillary tangle formation,⁶ pathophysiological symptoms present in osteomalacia, endemic amyotrophic lateral sclerosis, renal dialysis related encephalopathy, and other diseases.^{7,8} Gallium has been found to accumulate in biological tissues of tumorous nature, thus raising the possibility of its use in radiodiagnostic medicine for the

* To whom correspondence should be addressed. Tel: +30-81-393-652. Fax: +30-81-393-601. E-mail: salif@chemistry.uoh.gr.

[†] University of Crete.

[‡] Institute of Materials Science, NRCPS "Demokritos".

[§] University of Szeged.

^{||} Kossuth University.

[⊥] Michigan State University.

[⊗] National Hellenic Research Foundation, Institute of Organic and Pharmaceutical Chemistry.

(1) Martin, R. B. *Acc. Chem. Res.* **1994**, *27*, 204–210.

(2) (a) Anghileri, L. J.; Maleki, P.; Cordova Martinez, A.; Crone-Escanye, M. C.; Robert, J. *Nuklearmedizin* **1991**, *30*, 290–293. (b) Vallabhajosula, S.; Goldsmith, S. J.; Lipszyc, H.; Chahinian, A. P.; Ohnuma, T. *Eur. J. Nucl. Med.* **1983**, *8*, 354–357.

(3) (a) Radunovic, A.; Delves, H. T.; Bradbury, M. W. *Biol. Trace Elem. Res.* **1998**, *62*, 51–64. (b) Cochran, M.; Neoh, S.; Stephens, E. *Clin. Chim. Acta* **1983**, *132*, 199–203. (c) Nikpoor, N.; Drum, D. E.; Aliabadi, P. *J. Nucl. Med.* **1992**, *33*, 643–645.

(4) (a) Wang, S.; Lee, R. J.; Mathias, C. J.; Green, M. A.; Low, P. S. *Bioconjug. Chem.* **1996**, *7*, 56–62. (b) Anghileri, L. J. *Int. J. Rad. Appl. Instrum. [B]* **1991**, *18*, 259–260. (c) Harris, A. W.; Sephton, R. G. *Cancer Res.* **1977**, *37*, 3634–3638.

(5) (a) Forbes, W. F.; Agwani, N. *J. Theor. Biol.* **1994**, *171*, 207–214. (b) Flaten, T. P.; Garruto, R. M. *J. Theor. Biol.* **1992**, *156*, 129–132. (c) Exley, C.; Birchall, J. D. *J. Theor. Biol.* **1992**, *159*, 83–98.

(6) (a) Clauber, M.; Joshi, J. G. *Proc. Natl. Acad. Sci. U.S.A.* **1993**, *90*, 1009–1012. (b) Fasman, G. D.; Moore, C. D. *Proc. Natl. Acad. Sci. U.S.A.* **1994**, *91*, 11232–11235. (c) Vyas, S. B.; Duffy, L. K. *Biochem. Biophys. Res. Commun.* **1995**, *206*, 718–723.

localization, imaging, and treatment of aberrant soft tissue.⁹ In both cases, the involvement of citric acid^{9,10,11} has been noted to influence the accumulation and bioavailability of Al(III) and Ga(III) ions. Citric acid, a tricarboxylic acid, is amply distributed in the human plasma (0.1 mM) and serves as the most prevalent metal ion binder in plasma.¹² Citrate has also been linked with elevated absorption and toxic effects of aluminum in biological tissues^{13,14} and has been noted to contribute to gallium's accumulation in soft tumor tissue.¹⁵

Studies of Al(III) and Ga(III) in aqueous media, in the presence of citrate,^{11d,16,17} have thus far been aimed at unraveling their speciation patterns, but structural information about aluminum(gallium)-citrate species in aqueous solution has been scarce. Complexes of other metals such as iron,¹⁸ chromium,¹⁹ and copper²⁰ have been synthesized and characterized. Lately, aluminum-citrate²¹ and gallium complexes²² have been reported in the literature, signifying the emergence of a burgeoning synthetic field in the area. Herein, we report on studies, aimed at the synthesis, crystallographic, and spectroscopic characterization of low molecular weight, soluble aluminum and gallium-citrate species, their pH dependent structural diversity, their dynamic solution structures and transformations, and their potential relevance to biological systems.

Experimental Section

Materials and Methods. All reactions, reported in this work, were carried out in the air and at room temperature. The chemicals were purchased from Aldrich Chemical Co. The water was of nano-pure quality. Absolute ethanol was purchased from Riedel-de-Haën. D₂O, DCl, and NaOD were all Sigma products. The FT-infrared spectra were recorded on a Perkin-Elmer 1760X Fourier transform infrared spectrometer, in KBr pellets. Elemental analyses were carried out by Quantitative Technologies, Inc.

- (7) (a) Van der Voet, G. B.; Van Ginkel, M. F.; de Wolff, F. A. *Tox. Appl. Pharm.* **1989**, *99*, 90–97. (b) Kerr, D. N. S.; Ward, M. K. In *Metal Ions in Biological Systems*; Sigel, H.; Sigel, A., Eds.; Marcel Dekker: New York, 1988; Vol. 24, pp 217–258.
- (8) van Breemen, N. *Nature* **1985**, *315*, 16.
- (9) (a) Edwards, C. L.; Hayes, R. L. *J. Am. Med. Assoc.* **1970**, *212*, 1182–1191. (b) Edwards, C. L.; Hayes, R. L. *J. Nucl. Med.* **1969**, *10*, 103–105.
- (10) (a) Domingo, J. L.; Gomez, M.; Llobet, J. M.; del Castillo, D.; Corbella, J. *Nephron* **1994**, *66*, 108–109. (b) Öhman, L.-O.; Martin, R. B. *Clin. Chem.* **1994**, *40*, 598–601.
- (11) (a) McGregor, S. J.; Brock, J. H. *Clin. Chem.* **1992**, *38*, 1883–1885. (b) Kohno, H.; Katoh, S.; Ohkubo, Y.; Kubodera, A. *Radioisotopes* **1990**, *39*, 20–23. (c) Kohno, H.; Ohkubo, Y.; Kubodera, A. *Radioisotopes* **1987**, *36*, 523–525. (d) Glickson, J. D.; Pitner, T. P.; Webb, J.; Gams, R. A. *J. Am. Chem. Soc.* **1975**, *97*, 1679–1683. (e) Glickson, J. D.; Webb, J.; Gams, R. A. *Cancer Res.* **1974**, *34*, 2957–2960. (f) Glickson, J. D.; Ryel, R. B.; Bordenca, M. B.; Kim, K. H.; Gams, R. A. *Cancer Res.* **1973**, *33*, 2706–2713.
- (12) (a) Martin, R. B. *Inorg. Biochem.* **1986**, *28*, 181–187. (b) Glusker, J. P. *Acc. Chem. Res.* **1980**, *13*, 345–352.
- (13) (a) Slanina, P.; Frech, W.; Ekström, L.-G.; Löf, L.; Slorach, S.; Cedrgren, A. *Clin. Chem.* **1986**, *32*, 539–541. (b) Weberg, R.; Berstad, A. *Eur. J. Clin. Invest.* **1986**, *16*, 428–432.
- (14) Kirschbaum, B. B.; Schoolworth, A. C. *The Am. J. Med. Sci.* **1989**, *297*, 9–11.
- (15) Jonkhoff, A. R.; Plaizier, M. A. B. D.; Ossenkoppele, G. J.; Teule, G. J. J.; Huijgens, P. C. *Brit. J. Cancer* **1995**, *72*, 1541–1546.
- (16) (a) Venturini, M.; Berthon, G. *J. Inorg. Biochem.* **1989**, *37*, 69–90. (b) Öhman, L.-O. *Inorg. Chem.* **1988**, *27*, 2565–2570. (c) Gregor, J. E.; Powell, H. K. *Aust. J. Chem.* **1986**, *39*, 1854–1864. (d) Motekaitis, R. J.; Martell, A. E. *Inorg. Chem.* **1984**, *23*, 18–23. (e) Öhman, L.-O.; Sjöberg, S. J. *J. Chem. Soc., Dalton Trans.* **1983**, 2513–2517. (f) Karlik, S. J.; Tarien, E.; Elgavish, G. A.; Eichhorn, G. L. *Inorg. Chem.* **1983**, *22*, 525–529.
- (17) (a) Jackson, G. E. *Polyhedron* **1990**, *9*, 163–170. (b) Clevette, D. J.; Orvig, C. *Polyhedron* **1990**, *9*, 151–161. (c) Taylor, M. J. *Polyhedron* **1990**, *9*, 207–214. (d) Harris, W. R.; Martell, A. E. *Inorg. Chem.* **1976**, *15*, 713–720.

The high-resolution solid-state ¹³C Magic Angle Spinning (MAS) NMR spectra were measured at 100.63 MHz, on a Bruker MSL400 NMR spectrometer, capable of high power ¹H-decoupling. The spinning rate used for ¹H–¹³C cross polarization and magic angle spinning experiments was 5 kHz at ambient temperature (25 °C). Each solid-state spectrum was a result of the accumulation of 200 scans. The recycle delay used was 4 s, the 90° pulse was 5 μs, and the contact time was 1 ms. All solid-state spectra were referenced to adamantane, which showed two peaks at 26.5 and 37.6 ppm, respectively. The samples for solution NMR studies were prepared by dissolving the crystalline complexes in D₂O, at concentrations in the range 0.02–0.10 M. In D₂O solutions, the pD (pH meter reading +0.40) was adjusted with concentrated DCl and NaOD solutions. NMR spectra were recorded on Bruker AM360 (¹H, ¹³C, and ²⁷Al) and AM500 (²⁷Al) spectrometers. Chemical shifts (δ) are reported in ppm relative to internal DSS (¹³C and ¹H) and external [Al(H₂O)₆]³⁺ (²⁷Al) references. The ¹H-COSY spectrum was measured on a Bruker AM360 spectrometer, using the standard Bruker microprogram.

Preparations

(NH₄)₅{Al^{III}(C₆H₄O₇)₂}·2H₂O (MW = 529.41) (**1**). A mixture of 0.20 g (0.53 mmol) Al(NO₃)₃·9H₂O and 0.22 g (1.06 mmol) citric acid monohydrate was dissolved in 10 mL of water. The resulting slurry was stirred at 40–50 °C overnight, during which time both reactants went into solution. The color of the solution remained clear throughout that period. On the following day, the water was removed by means of a rotary evaporator. The produced gummy material was redissolved in a minimum amount of water, and the pH was adjusted to ~8 with aqueous ammonia. Addition of absolute ethanol at 4 °C yielded crystalline material, which was isolated by filtration. The yield was 0.14 g (49.6%). Anal. Calcd for C₁₂H₃₂O₁₆N₅Al: C, 27.20; H, 6.04; N, 13.22. Found: C, 26.96; H, 5.83; N, 12.91.

Under similar reaction conditions, in the presence of Al(NO₃)₃·9H₂O and citric acid anhydrous with a 1:1 molar ratio, a material identical to that obtained with the 1:2 molar ratio was isolated. Positive identification was provided by FT-IR (yield 25.5%).

(NH₄)₅{Ga^{III}(C₆H₄O₇)₂}·2H₂O (MW = 572.14) (**2**). Preparation of the gallium analogue was carried out by the same procedure as in the case of complex **1**. The amounts of reactants used were 0.38 g (1.48 mmol) of Ga(NO₃)₃·xH₂O and 0.57 g (2.97 mmol) of citric acid anhydrous. The yield was 0.40 g (47.1%). Anal. Calcd for C₁₂H₃₂N₅O₁₆Ga: C, 25.16; H, 5.59; N, 12.24. Found: C, 24.83; H, 5.40; N, 12.56.

(NH₄)₄{Al^{III}(C₆H₄O₇)(C₆H₅O₇)}·3H₂O (MW = 530.39) (**3**). A 0.20 g (0.53 mmol) amount of Al(NO₃)₃·9H₂O and 0.22 g (1.06 mmol) of citric acid monohydrate were dissolved in 10 mL of nano-pure water. The resulting slurry was stirred at 50 °C overnight. On the following day, the solution was taken to dryness by means of a rotary evaporator. The produced gummy material was redissolved in a minimum amount of water, and the pH was adjusted to ~4.5 with aqueous ammonia. Addition of absolute ethanol at 4 °C yielded crystalline material, which

- (18) (a) Matzapetakis, M.; Raptopoulou, C. P.; Tsohos, A.; Papefthymiou, B.; Moon, N.; Salifoglou, A. *J. Am. Chem. Soc.* **1998**, *120*, 13266–13267. (b) Shweky, I.; Bino, A.; Goldberg, D. P.; Lippard, S. J. *Inorg. Chem.* **1994**, *33*, 5161–5162.
- (19) Quiros, M.; Goodgame, D. M. L.; Williams, D. J. *Polyhedron* **1992**, *11*, 1343–1348.
- (20) Bott, R. C.; Sagatys, D. S.; Lynch, D. E.; Smith, G.; Kennard, C. H. L.; Mak, T. C. W. *Aust. J. Chem.* **1991**, *44*, 1495–1498.
- (21) (a) Matzapetakis, M.; Raptopoulou, C. P.; Terzis, A.; Lakatos, A.; Kiss, T.; Salifoglou, A. *Inorg. Chemistry* **1999**, *38*, 618–619. (b) Feng, T. L.; Gurian, P. L.; Healy, M. D.; Barron, A. R. *Inorg. Chem.* **1990**, *29*, 408–411.
- (22) O'Brien, P.; Salacinski, H.; Motevalli, M. *J. Am. Chem. Soc.* **1997**, *119*, 12695–12696.

was isolated by filtration. The yield was 0.25 g (88.4%). Anal. Calcd for $C_{12}H_{31}O_{17}N_4Al$: C, 27.15; H, 5.84; N, 10.56. Found: C, 26.98; H, 5.95; N, 10.23.

(NH₄)₄{Ga^{III}(C₆H₄O₇)(C₆H₅O₇)}·3H₂O (MW = 573.13) (4). Preparation of the gallium analogue was carried out by the same procedure as in the case of complex **3**. The amounts of reactants used were 0.20 g (0.78 mmol) of Ga(NO₃)₃·xH₂O and 0.30 g (1.56 mmol) of citric acid anhydrous. The yield was 0.14 g (31.1%). Anal. Calcd for $C_{12}H_{31}O_{17}N_4Ga$: C, 25.13; H, 5.41; N, 9.77. Found: C, 25.21; H, 5.39; N, 9.81.

K₄{Al^{III}(C₆H₄O₇)(C₆H₅O₇)}·4H₂O (MW = 632.64) (5). The preparation was carried out by the same procedure as in the case of complex **3**. The amounts of reactants used were 0.20 g (0.53 mmol) of Al(NO₃)₃·9H₂O and 0.20 g (1.05 mmol) of citric acid anhydrous. A solution of KOH was used to adjust the pH of the reaction mixture between 4.5 and 6. The yield was 0.18 g (~30%). Anal. Calcd for $C_{12}H_{17}K_4O_{18}Al$: C, 22.76; H, 2.69; K, 24.72. Found: C, 22.89; H, 2.62; K, 24.53.

K₄{Ga^{III}(C₆H₄O₇)(C₆H₅O₇)}·4H₂O (MW=675.38) (6). Preparation of the gallium analogue was carried out by the same procedure as in the case of complex **3**. The amounts of reactants used were 0.38 g (1.48 mmol) of Ga(NO₃)₃·xH₂O and 0.57 g (2.97 mmol) of citric acid anhydrous. A solution of KOH was used to adjust the pH of the reaction mixture between 4.5 and 6. The yield was 0.25 g (25%). Anal. Calcd for $C_{12}H_{17}K_4O_{18}Ga$: C, 21.32; H, 2.52; K, 23.16. Found: C, 21.48; H, 2.47; K, 23.22.

Interconversions

Compound 1 and Compound 3. A 0.13 g (0.24 mmol) amount of **1** was dissolved in 5 mL of water at pH ~8. The solution was adjusted to pH ~4.5 by adding HNO₃ (1:1 dilution with water) dropwise, over a period of 2 h. The resulting solution was stirred for a few more hours at room temperature. Subsequently, ethanol was added and the flask containing the mixture was placed at 4 °C. Ten days later crystalline material came out of solution, which was isolated by filtration, and dried in vacuo. The FT-IR spectrum (in KBr) of the isolated crystals was identical to that of **3**. The yield was 0.08 g (0.15 mmol, 61.2%).

Under similar reaction conditions, **3** was found to convert to compound **1** by adjusting the solution pH to ~8 with aqueous ammonia. The FT-IR spectrum (in KBr) of the isolated crystals was identical to that of **1**. The yield was 40.0%.

Compound 2 and Compound 4. The same procedure was employed here as in the case of the conversion of complex **1** to **3**. The amount of **2** used was 0.08 g (0.14 mmol). The FT-IR spectrum (in KBr) of the isolated crystals was identical to that of **4**. The yield of the conversion reaction was 0.03 g (0.05 mmol, 35.7%).

Under similar reaction conditions, **4** was found to convert to **2** by adjusting the solution pH to ~8 with aqueous ammonia. The FT-IR spectrum (in KBr) of the isolated crystals was identical to that of **2**. The yield was 25.0%.

X-ray Crystal Structure Determination. X-ray quality crystals of compounds **1–6** were grown from water–ethanol mixtures. Crystallographic details for **1** have been previously reported.^{21a} Data collection for **2** (0.10 × 0.10 × 0.40 mm) was carried out on a Crystal Logic dual-goniometer diffractometer, whereas data collection for **3** (0.10 × 0.20 × 0.20 mm) and **4** (0.10 × 0.20 × 0.30 mm) was carried out on a P2₁ Nicolet diffractometer, upgraded by Crystal Logic, using θ – 2θ scans. During data collection, three standard reflections were monitored every 97 reflections and showed less than 3% variation and no

decay. Lorentz, polarization, and psi-scan absorption corrections were applied by using Crystal Logic software. Further crystallographic details: for **2**, $2\theta_{\max} = 50^\circ$; scan speed 4.2°/min; scan range $2.5 + \alpha_1\alpha_2$ separation; reflections collected/unique/used, 2168/1997 [$R_{\text{int}} = 0.0196$]/1997; 225 parameters refined; $[\Delta/\sigma]_{\max} = 0.023$; $[\Delta\rho]_{\max}/[\Delta\rho]_{\min} = 0.561/-0.452$ e/Å³; R/R_w (for all data), 0.0285/0.0755; for **3**, $2\theta_{\max} = 130^\circ$; scan speed 3.0°/min; scan range $2.3 + \alpha_1\alpha_2$ separation; reflections collected/unique/used, 3830/3724 [$R_{\text{int}} = 0.0106$]/3724; 433 parameters refined; $[\Delta/\sigma]_{\max} = 0.009$; $[\Delta\rho]_{\max}/[\Delta\rho]_{\min} = 0.723/-0.483$ e/Å³; R/R_w (for all data), 0.0434/0.1056; for **4**, $2\theta_{\max} = 130^\circ$; scan speed 3.0°/min; scan range $2.5 + \alpha_1\alpha_2$ separation; reflections collected/unique/used, 6809/3767 [$R_{\text{int}} = 0.0124$]/3767; 433 parameters refined; $[\Delta/\sigma]_{\max} = 0.011$; $[\Delta\rho]_{\max}/[\Delta\rho]_{\min} = 0.703/-0.315$ e/Å³; R/R_w (for all data), 0.0277/0.0661. Data collection for **5** (0.13 × 0.08 × 0.08 mm) and **6** (0.13 × 0.13 × 0.10 mm) was carried out on a Bruker (formerly Siemens) SMART Platform CCD diffractometer, using ω scans. Almost a full sphere of data (1960 frames) was collected for **6**, while a little over a hemisphere of data (1277 frames) was collected for **5**. Final cell constants were calculated from a set of 2957 and 1278 strong reflections obtained from the data collection of **6** and **5**, respectively. In both data collections, 3–4 different sets of frames were collected using 0.30° steps in ω . The detector-to-crystal distance was ~5 cm. Further crystallographic details: for **5**, $2\theta_{\max} = 56.5^\circ$; exposure time = 50 s per frame; reflections collected/unique/used, 3166/2359 [$R_{\text{int}} = 0.0249$]/2359; 193 parameters refined; $[\Delta/\sigma]_{\max} = 0.001$; $[\Delta\rho]_{\max}/[\Delta\rho]_{\min} = 0.398/-0.327$ e/Å³; R/R_w (for all data), 0.0607/0.0932; for **6**, $2\theta_{\max} = 57.8^\circ$; exposure time = 35 s per frame; reflections collected/unique/used, 5232/2534 [$R_{\text{int}} = 0.0231$]/2534; 193 parameters refined; $[\Delta/\sigma]_{\max} = 0.001$; $[\Delta\rho]_{\max}/[\Delta\rho]_{\min} = 0.390/-0.400$ e/Å³; R/R_w (for all data), 0.0365/0.0620. The SMART^{23a} software was used for data acquisition, and SAINT^{23b} was used for data extraction. Lorentz, polarization, and absorption corrections were applied by using SADABS.^{23c}

The structures of **2–4** were solved by direct methods using SHELXS-86^{24a} and refined by full-matrix least-squares techniques on F^2 by using SHELXL93.^{24b} The structure of **6** was solved by direct methods using teXsan²⁵ and refined with the aid of full-matrix least-squares techniques on F^2 by using the SHELXTL^{26a} and/or SHELX97^{26b} programs. The structure of **5** was refined using the coordinates of its isostructural congener **6**. All non-H atoms were refined anisotropically. All H-atoms were located by difference maps and refined isotropically. In the crystal structure of **2**, N3 occupies a center of symmetry. Therefore, the ammonium ion is disordered. Only three of the four hydrogen atoms were located in the difference Fourier map. In the crystal structures of **3** and **4**, the N4 and N5 atoms of the ammonium counterions sit on a C₂ axis of symmetry at 0.25,y,0.50 and 0.75,y,0.0, respectively. Therefore, only two of their hydrogen atoms are crystallographically independent. A summary of crystallographic data is given in

- (23) (a) SMART v5.054; Bruker Analytical X-ray Systems Inc.: Madison, WI 53719, 1999. (b) SAINT v6.01; Bruker Analytical X-ray Systems Inc.: Madison, WI 53719, 1999. (c) Sheldrick, G. M. SADABS; University of Göttingen: Germany.
- (24) (a) Sheldrick, G. M. SHELXS-86: Structure Solving Program; University of Göttingen: Germany, 1986. (b) Sheldrick, G. M. SHELXL93: Structure Refinement Program; University of Göttingen: Germany, 1993.
- (25) teXsan v1.8; Molecular Structure Corporation: The Woodlands, TX 77831, 1996.
- (26) (a) SHELXTL v5.1; XBruker Analytical X-ray Systems Inc.: Madison, WI 53719, 1999. (b) Sheldrick, G. M. SHELX97; University of Göttingen: Germany.

Table 1. Summary of Crystal, Intensity Collection and Refinement Data for Compounds (NH₄)₅{Al(C₆H₄O₇)₂}·2H₂O (1), (NH₄)₅{Ga(C₆H₄O₇)₂}·2H₂O (2), (NH₄)₄{Al(C₆H₅O₇)(C₆H₄O₇)}·3H₂O (3), (NH₄)₄{Ga(C₆H₅O₇)(C₆H₄O₇)}·3H₂O (4), K₄{Al(C₆H₅O₇)(C₆H₄O₇)}·4H₂O (5), and K₄{Ga(C₆H₅O₇)(C₆H₄O₇)}·4H₂O (6)

	1	2	3	4	5	6
chemical formula	C ₁₂ H ₃₂ N ₅ O ₁₆ Al	C ₁₂ H ₃₂ N ₅ O ₁₆ Ga	C ₁₂ H ₃₁ N ₄ O ₁₇ Al	C ₁₂ H ₃₁ N ₄ O ₁₇ Ga	C ₁₂ H ₁₇ K ₄ O ₁₈ Al	C ₁₂ H ₁₇ K ₄ O ₁₈ Ga
formula weight	529.41	572.14	530.39	573.13	632.64	675.38
temperature, °C	25	25	25	25	25	-100
wavelength, λ (Å)	Mo K _α 0.71073	Mo K _α 0.71073	Cu K _α 1.54180	Cu K _α 1.54180	Mo K _α 0.71073	Mo K _α 0.71073
space group	P1	P1	I2/a	I2/a	P1	P1
a (Å)	9.638(5)	9.659(6)	19.347(3)	19.275(1)	7.316(1)	7.3242(2)
b (Å)	9.715(5)	9.762(7)	9.857(1)	9.9697(6)	9.454(2)	9.4363(5)
c (Å)	7.237(4)	7.258(5)	23.412(4)	23.476(1)	9.569(2)	9.6435(5)
α, deg	90.96(1)	90.95(2)			64.218(4)	63.751(2)
β, deg	105.72(1)	105.86(2)	100.549(5)	100.694(2)	69.872(3)	70.091(2)
γ, deg	119.74(1)	119.28(1)			69.985(4)	69.941(2)
V, (Å ³)	557.1(3)	564.9(7)	4389(1)	4432.8(5)	544.9(2)	547.22(4)
Z	1	1	8	8	1	1
ρ _{calcd} /ρ _{obsd} (g/cm ³)	1.578/1.55	1.681/1.66	1.605/1.58	1.718/1.69	1.928	2.049
abs. coeff (μ), cm ⁻¹	1.80	13.06	16.73	25.54	9.47	21.08
R ^a	0.0498	0.0281	0.0389	0.0250	0.0398	0.0267
R _w ^a	0.1477 ^b	0.0749 ^c	0.1010 ^d	0.0640 ^e	0.0873 ^f	0.0604 ^g

^a R values are based on F², R_w values are based on F²; $R = \sum ||F_o| - |F_c|| / \sum |F_o|$, $R_w = \sqrt{\sum [w(F_o^2 - F_c^2)^2] / \sum [w(F_o^2)^2]}$. ^b For 1494 reflections with $I > 2\sigma(I)$. ^c For 1967 reflections with $I > 2\sigma(I)$. ^d For 3362 reflections with $I > 2\sigma(I)$. ^e For 3495 reflections with $I > 2\sigma(I)$. ^f For 1725 reflections with $I > 2\sigma(I)$. ^g For 2048 reflections with $I > 2\sigma(I)$.

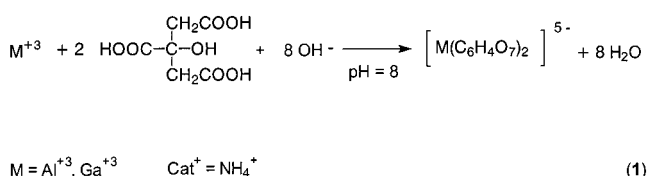
Table 2. Bond Lengths (Å) and Angles (deg) for Compounds (NH₄)₅{Al(C₆H₄O₇)₂}·2H₂O (1), (NH₄)₅{Ga(C₆H₄O₇)₂}·2H₂O (2), (NH₄)₄{Al(C₆H₅O₇)(C₆H₄O₇)}·3H₂O (3), (NH₄)₄{Ga(C₆H₅O₇)(C₆H₄O₇)}·3H₂O (4), K₄{Al(C₆H₅O₇)(C₆H₄O₇)}·4H₂O (5), and K₄{Ga(C₆H₅O₇)(C₆H₄O₇)}·4H₂O (6)

	1	2	3	4	5	6
M—O(3)	1.844(3)	1.902(2)	1.836(1)	1.893(1)	1.821(2)	1.8812(13)
M—O(13)			1.846(1)	1.900(1)		
M—O(5)	1.884(3)	1.966(2)	1.899(1)	1.976(1)	1.915(2)	1.9912(14)
M—O(15)			1.904(1)	1.983(1)		
M—O(1)	1.961(3)	2.056(2)	1.937(2)	2.022(1)	1.954(2)	2.0418(14)
M—O(11)			1.959(1)	2.058(1)		
O(3)—M—O(13)			177.18(6)	176.57(5)		
O(13)—M—O(5)			94.03(6)	95.34(5)		
O(3)—M—O(5)	85.64(13)	84.36(8)	85.88(6)	84.57(5)	85.87(7)	84.75(6)
O(13)—M—O(15)			85.58(6)	84.40(5)		
O(3)—M—O(15)			94.47(6)	95.61(5)		
O(5)—M—O(15)			179.23(6)	178.67(5)		
O(3)—M—O(1)	89.70(11)	89.27(7)	90.33(6)	90.15(5)	90.46(7)	90.78(6)
O(13)—M—O(1)			92.49(6)	93.28(5)		
O(5)—M—O(1)	89.45(10)	89.09(7)	89.79(6)	89.46(6)	88.57(8)	88.27(6)
O(15)—M—O(1)			90.90(6)	91.86(6)		
O(3)—M—O(11)			88.56(6)	88.58(5)		
O(13)—M—O(11)			88.62(6)	87.99(5)		
O(5)—M—O(11)			89.49(6)	89.90(5)		
O(15)—M—O(11)			89.83(6)	88.78(5)		
O(1)—M—O(11)			178.72(6)	178.62(5)		

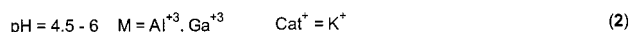
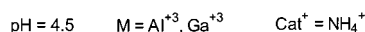
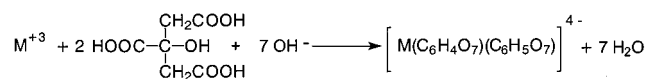
Table 1. Selected bond length and angle data for all structures are listed in Table 2.

Results

Syntheses. The syntheses of compounds 1–6 were expediently carried out in aqueous solutions, under varying pH conditions, with a 1:2 metal to citrate stoichiometry. Specifically, complexes 1 and 2 were synthesized at pH ~8 (reaction 1).



Complexes 3–6 were synthesized, by employing the same reagents as in reaction 1, at pH ~4.5 (reaction 2) for the NH₄⁺ salts, and at pH ~4.5–6 for the K⁺ salts.



In all cases, the resulting products precipitated out of solution in a crystalline form and were isolated by filtration. All of the complexes are soluble in water and highly insoluble in alcohols and other organic solvents (DMF, CH₃CN, toluene, etc.)

In view of the fact that an asymmetric trinuclear complex [Al₃(CitH₋₁)₃(OH)]⁴⁻ (21b) ((CitH₋₁)⁴⁻ = (C₆H₄O₇)⁴⁻) had been isolated from a reaction mixture with a 1:1 Al(III):citrate ratio, an investigation of the reactions run with Al(III) was also attempted with that same 1:1 ratio. As a result, the reaction product isolated at pH ~8 was the same, albeit with a lower yield, as the product of the reaction run with a 1:2 Al(III):citrate

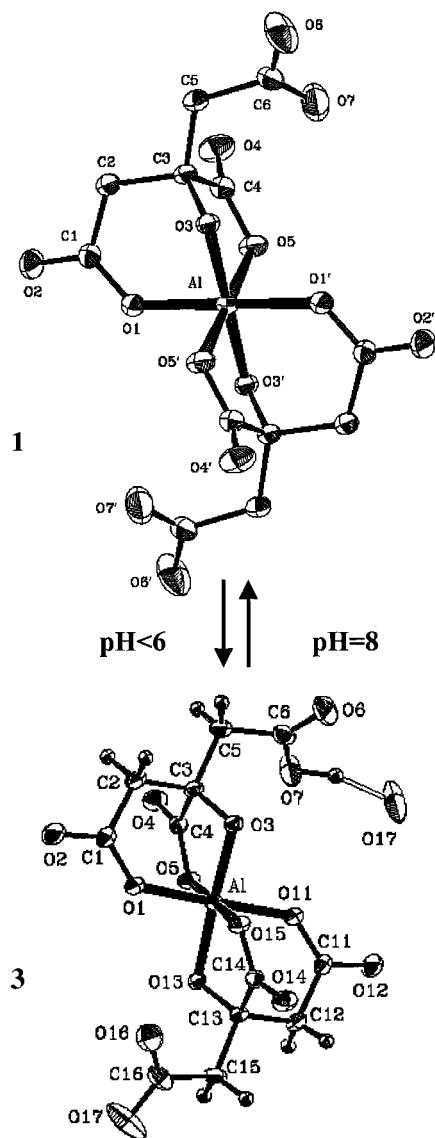


Figure 1. pH Interconversions between **1** and **3**. ORTEP diagrams of $[\text{Al}(\text{C}_6\text{H}_4\text{O}_7)_2]^{5-}$ (**1**) and $[\text{Al}(\text{C}_6\text{H}_4\text{O}_7)(\text{C}_6\text{H}_5\text{O}_7)]^{4-}$ (**3**) with thermal ellipsoids representing 50% probability surfaces.

ratio. Similar results were obtained with a 1:0.5 Al(III):citrate ratio (*not shown*). It appears, therefore, that under the conditions employed in the described reactions, the least soluble product, out of a mixture of potential equilibrium species purported to exist, is the 1:2 Al(III):citrate complex.

Use of various cations did not result in the isolation of different products. Thus, regardless of the cation used (NH_4^+ , K^+), the structure of the anion was the same in all complexes isolated under the specified pH and stoichiometric conditions, as that was judged by the X-ray crystallography results.

Reactivity Interconversions. Having synthesized and isolated compounds **1–6**, an effort was made to investigate the behavior of these species under varying pH conditions. In that respect, when **1** and **2** were placed in water, and the pH was gradually adjusted from ~ 8 to ~ 4.5 , precipitation with alcohol led to the isolation of **3** and **4**, respectively. Conversely, when compounds **3** and **4** were dissolved in water, and the pH of the resulting solution was gradually increased from ~ 4.5 to ~ 8 , addition of alcohol led to the isolation of **1** and **2**. Thus, in both directions, pH adjustment of the solutions containing the known isolated species, leads to the interconversion between **1** and **3**, and **2** and **4**, respectively (Figure 1). Attempts to isolate species at

pH values between 4.5 and 8 led to either one or the other complex, depending on the specific final solution pH value achieved.

Description of the Structures. $(\text{NH}_4)_5\text{M}(\text{C}_6\text{H}_4\text{O}_7)_2 \cdot 2\text{H}_2\text{O}$ ($\text{M} = \text{Al}(\text{III})$ (**1**), $\text{Ga}(\text{III})$ (**2**)). The X-ray crystal structures of **1** and **2** consist of centrosymmetric elongated octahedral complexes, with two citrate ligands bound to the M(III) (Al, Ga) ion. An ORTEP drawing of **1** is given in Figure 1. Each citrate ligand is fully deprotonated. As such, it coordinates to aluminum/gallium through its central alcoholate and carboxylate groups in the equatorial plane and through a terminal carboxylate in the axial position. The third terminal carboxylate group, also deprotonated, remains unbound. In both structures, the M–O (carboxylate) axial distances of 1.961(3) Å in **1**, and 2.056(2) Å in **2**, are slightly longer than the equatorial distances of 1.844–(3) Å (hydroxyl) and 1.884(3) Å (central carboxylate) in **1**, and 1.902(2) Å and 1.966(2) Å in **2**. The structural features of the octahedral coordination of citrate around Al(III) are similar to those observed in the previously reported trinuclear complex $[\text{Al}_3(\text{H}-1\text{Cit})_3(\text{OH})]^{4-}$.^{21b}

The Ga–O distances in **2** appear to be in the range of those observed in $\text{GaMe}_2(\text{trimethylcitrate})$ (1.950(3)–2.395(3) Å),²⁷ $(\text{NH}_4)_3[\text{Ga}(\text{C}_2\text{O}_4)_3] \cdot 3\text{H}_2\text{O}$ (1.961–1.976 Å),²⁸ $\text{Ga}(\text{C}_8\text{H}_{10}\text{NO}_2)_3 \cdot 12\text{H}_2\text{O}$ (1.962(1)–2.000(1) Å),²⁹ $\text{Ga}(\text{ptp})_3 \cdot 5.5\text{H}_2\text{O}$ (1.962(2)–1.996(2) Å),³⁰ $\text{Ga}(\text{mmb})_3$ (1.944(2)–1.989(2) Å),³¹ $[\text{Ga}_2(\beta\text{-D-mann/H}_-)_2]^{4-}$ (range: 1.955(3)–2.052(3) Å),³² and $\text{Ga}(\text{dpp})_3$ (range: 1.967(3)–1.990(3) Å).³³ In both **1** and **2**, the M–O distances are similar to those observed in other mononuclear metal citrate complexes such as $(\text{NH}_4)_5[\text{Fe}(\text{C}_6\text{H}_4\text{O}_7)_2] \cdot 2\text{H}_2\text{O}$ (1.953(2)–2.068(2) Å),¹⁸ $(\text{NH}_4)_3[\text{Ga}(\text{C}_6\text{H}_5\text{O}_7)_2] \cdot 4\text{H}_2\text{O}$ (1.890(2)–2.054(2) Å),²² and $(\text{pyH})_2[\text{Cr}(\text{cit})_2] \cdot 4\text{H}_2\text{O}$ (1.965(1)–1.987(2) Å).¹⁹ An extensive network of hydrogen bonds connects the complex anion with the NH_4^+ cations through mediating water molecules in the lattices of **1** and **2**.

$(\text{Cat})_4[\text{Al}(\text{C}_6\text{H}_4\text{O}_7)(\text{C}_6\text{H}_5\text{O}_7)] \cdot n\text{H}_2\text{O}$ [Cat. = NH_4^+ , $n = 3$ (**3**); Cat. = K^+ , $n = 4$ (**5**)]. The structure of the anion $[\text{Al}(\text{C}_6\text{H}_4\text{O}_7)(\text{C}_6\text{H}_5\text{O}_7)]^{4-}$ reveals the presence of an octahedral complex, with two citrate ligands coordinated to Al(III). An ORTEP drawing of **3** is given in Figure 1. In both **3** and **5**, one of the citrate ligands involved in the coordination of Al(III) is fully deprotonated, whereas the other one is triply deprotonated. The hydrogen on the triply deionized citrate resides on the terminal carboxylate group, which remains unbound. That hydrogen forms a hydrogen bond with the oxygen of the deprotonated unbound carboxylate group in an adjacent anion in the lattice. In this sense, this hydrogen-bonded structure extends throughout the lattice in the direction dictated by the conformation of the unbound carboxylate groups of the citrate ligands. The axial Al–O distances in the octahedra of both structures, 1.959(1) Å (**3**) and 1.954(2) Å (**5**), are slightly longer than the equatorial distances, 1.836(1)–1.904(1) Å (**3**) and 1.821(2)–1.915(2) Å (**5**), respectively. In both **3** and **5**, the M–O distances are in the range of those observed in all three

(27) Banta, G. A.; Rettig, S. J.; Storr, A.; Trotter, J. *Can. J. Chem.* **1985**, *63*, 2545–2549.

(28) Bulc, N.; Golic, L.; Siftar, J. *Acta Crystallogr.* **1984**, *C40*, 1829–1831.

(29) Nelson, W. O.; Rettig, S. J.; Orvig, C. *Inorg. Chem.* **1989**, *28*, 3153–3157.

(30) Zhang, Z.; Rettig, S. J.; Orvig, C. *Inorg. Chem.* **1991**, *30*, 509–515.

(31) Dietrich, A.; Fidelis, K. A.; Powell, D. R.; van der Helm, D.; Eng-Wilmot, D. L. *J. Chem. Soc., Dalton Trans.* **1991**, 231–239.

(32) Burger, J.; Gack, C.; Klüfers, P. *Angew. Chem., Int. Ed. Engl.* **1995**, *34*, 2647–2649.

(33) Nelson, W. O.; Karpishin, T. B.; Rettig, S. J.; Orvig, C. *Inorg. Chem.* **1988**, *27*, 1045–1051.

octahedral Al(III) ions of the trinuclear complex $[\text{Al}_3(\text{H}_{-1}\text{Cit})_3(\text{OH})]^{4-}$.^{21b} The angles around Al(III), for **3** and **5**, are in the range 85.58(6)–94.47(6)°. Therefore, regardless of the cation employed to crystallize the anion, the angles around aluminum are similar for the K^+ and NH_4^+ salts, and close to the ideal octahedral angles. Here, as well, a complex hydrogen-bonding network forms, involving the cations (especially in **3**, where $\text{Cat}^+ = \text{NH}_4^+$), the waters of crystallization, and the citrate oxygens.

$(\text{Cat})_4[\text{Ga}(\text{C}_6\text{H}_4\text{O}_7)(\text{C}_6\text{H}_5\text{O}_7)] \cdot n\text{H}_2\text{O}$ [$\text{Cat} = \text{NH}_4^+$, $n = 3$ (**4**); $\text{Cat} = \text{K}^+$, $n = 4$ (**6**)]. The crystal structure of the anion $[\text{Ga}(\text{C}_6\text{H}_4\text{O}_7)(\text{C}_6\text{H}_5\text{O}_7)]^{4-}$ consists of an octahedral assembly of two citrate ligands bound to Ga(III). As in the case of the corresponding aluminum complexes, one of the citrates is quadruply deprotonated, while the other one acts as a triply deionized entity. Here as well, the hydrogen of the triply deprotonated citrate resides on an unbound terminal carboxylate, and is in a position to form a hydrogen bond with the oxygen of a terminal carboxylate in an adjacent anionic complex in the lattice. As a result of the ionic status of the citrate ligands, the overall charge of the complexes is 4–, in contrast to the charge of 5– in **1** and **2**, isolated at higher pH values. The Ga–O axial distances in **4** and **6** are slightly longer (2.022(1)–2.058(1) Å) than those in the equatorial plane (1.893(1)–1.983(1) Å). The angles around Ga(III) for **4** and **6** are in the range 84.40(5)–95.61(5)°.

O'Brien and co-workers²² have reported the crystal structure of $(\text{NH}_4)_3[\text{Ga}(\text{C}_6\text{H}_5\text{O}_7)_2] \cdot 4\text{H}_2\text{O}$ with the same crystal parameters as compound **4**, which we formulate as $(\text{NH}_4)_4[\text{Ga}(\text{C}_6\text{H}_5\text{O}_7)(\text{C}_6\text{H}_4\text{O}_7)] \cdot 3\text{H}_2\text{O}$. The difference is that in their case, both of the pendant carboxylates are protonated, while in **4** only one is protonated. As a consequence of having to balance the charges, they consider the two observed electron density peaks on the 2-fold axis as water oxygen atoms (O2W, O3W), while in **4** these peaks are considered as ammonium nitrogens (N4, N5). There are several reasons why, we believe, the herein-proposed formulation is the correct one. Two of the main reasons are the following: (1) A hydrogen position is not observed on one of the pendant carboxylates. On the other carboxylate group, a second hydrogen position is observed on both N4 and N5, so that through the action of the 2-fold axis, N4 and N5 give rise to nice tetrahedral ammonium ions. (2) The distance between H(14O) (which exists) and H(9O) ($x = 0.5, -y, z$) (which we claim does not exist) is 1.56 Å, which is not acceptable. Furthermore, the aforementioned structural behavior is also observed in compound **3**, which is isostructural to **4**.

Infrared Spectra. The FT-IR spectra of the title compounds, in KBr, were dominated by strong absorptions of the coordinated citrate carboxylate ligands in the carbonyl region. Specifically, distinct antisymmetric stretching vibrations, $\nu_{\text{as}}(\text{COO}^-)$, appeared between 1627 and 1588 cm^{-1} for **1**–**6**. The corresponding symmetric stretches, $\nu_{\text{s}}(\text{COO}^-)$, appeared in the range 1436–1380 cm^{-1} for **1**–**6**. For all compounds, the quoted observed bands were shifted to lower frequencies compared to those of free citric acid. Moreover, the difference $\Delta(\nu_{\text{as}}(\text{COO}^-) - \nu_{\text{s}}(\text{COO}^-))$ ³⁴ was consistently greater than 200 cm^{-1} for **1**–**6**, indicating the presence of deprotonated carboxylate groups, in the respective structures, that are either free or coordinated to the metal ion in a monodentate fashion. This observation was in agreement with the coordination mode of the citrate ligand in the X-ray crystal structures of **1**–**6**.

Solid-State NMR spectroscopy. The MAS ¹³C NMR

Table 3. NMR Spectral Parameters of the Al(III) Complexes **1** and **3** in the Solid State and in 0.1 M Solutions in D₂O, at $t = 25$ °C. "Bound" Citrate Pertains to the 1:2 Complex

method	complex 1			complex 3			
	solid state	solution (citrate)		solid state	solution (citrate)		
		free	bound		free	bound	
¹ H NMR		2.52	2.50		2.55	2.59	
		2.56	2.55		2.59	2.64	
		2.64	2.62		2.66	2.70	
		2.68	2.67		2.70	2.75	
¹³ C NMR	CH ₂	47.9	46.2	46.0	46.5, 48sh	45.8	n.o. ^a
	C	75.8	75.7	74.7	76.0	75.4	n.o.
	CO	178.2	179.7	179.6	177.5, 172.5	179.1	n.o.
		188.3	182.4	187.5	184.5, 189.0	181.9	n.o.

^a n.o. = not observed clearly.

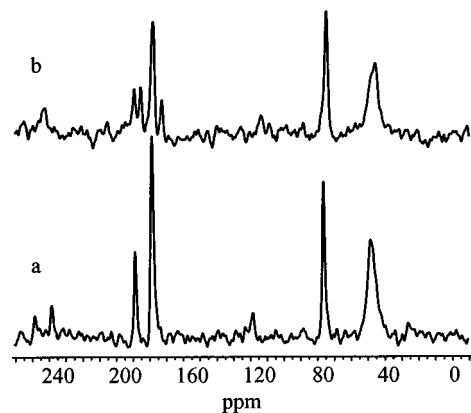


Figure 2. ¹³C-MAS NMR spectra of the solid Al(III) complexes. (a) **1** prepared at pH 8.0 and (b) **3** prepared at pH 4.5.

spectrum of **1** was consistent with the nonsymmetrical coordination mode of its Al(III)-bound citrate ligands, although not all peaks were fully resolved (Table 3): it showed four separate resonances, two in the high field region, and two in the carbonyl region (Figure 2a). Peaks in the high field region could, thus, be assigned to the CH₂ carbons (δ 47.9 ppm, a broad band of overlapping peaks of methylene carbons adjacent to bound and unbound carboxylates), and to the central carbon (δ 75.8 ppm, adjacent to the central bound carboxylates). In the carbonyl region, because of the poor resolution, only one signal (δ 178.2 ppm) was observed for the bound and unbound terminal carboxylate carbonyls. One signal was also observed for the central carboxylate carbonyl that is shifted to low field by about 11 ppm (δ 188.3 ppm), due to the presence of the neighboring ionized alkoxy group. Recently, Barrie et al.³⁵ reported the solid-state ¹³C spectrum of $\text{Na}_2[\text{Bi}_2(\text{CitH}_{-1})_2] \cdot 7\text{H}_2\text{O}$, which showed a very similar pattern, but with fully resolved resonances for the carbons of the two variably bound CH₂COO⁻ moieties (one is bound as a bidentate ligand to the metal ion, while the other one binds in a bridging mode to two metal ions).

The solid-state ¹³C NMR spectrum of **3** showed (Figure 2b) broadened or split resonances, due to the protonation of one of the unbound carboxylates. As a result, resonances for the methylene carbons became chemically distinguishable. Thus, a significantly broadened resonance was observed at 46.5 ppm, with a shoulder appearing around 48 ppm. Splitting of the resonance was also observed, for the terminal carboxylates, to

(34) (a) Djordjevic, C.; Lee, M.; Sinn, E. *Inorg. Chem.* **1989**, *28*, 719–723. (b) Deacon, G. B.; Philips, R. *J. Coord. Chem. Rev.* **1980**, *33*, 227–250.

(35) Barrie, P. J.; Djuran, M. I.; Mazid, M. A.; McPartlin, M.; Sadler, P. J.; Scowen, I. J.; Sun, H. *J. Chem. Soc., Dalton Trans.* **1996**, 2417–2422.

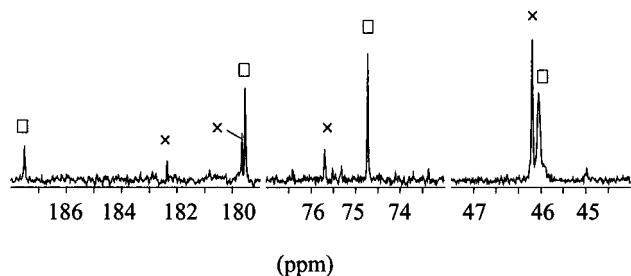


Figure 3. ^{13}C NMR spectrum of a 0.1 M solution of **1** in D_2O 1 h following dissolution, pD = 8.3. Labels: (x), free citrate; (□), citrate complexed in the 1:2 complex.

peaks with a 3:1 intensity ratio at δ 177.5 and 172.5 ppm, as well as for the central carboxylate carbonyls to peaks with a 1:1 intensity ratio at δ 189.0 and 184.5 ppm, respectively. The splitting of the bound central carboxylate carbonyl peaks may arise from protonation of one of the unbound terminal carboxylates and might be a consequence of an interaction not unlike one promoted by hydrogen-bonding.

The MAS ^{13}C NMR spectra of the Ga(III) complexes **2** and **4** were very similar to those of the corresponding Al(III) complexes **1** and **3** (Tables 3 and 4). This similarity suggested similar structures for both pairs of compounds in the solid state. This conclusion was strongly corroborated by the X-ray crystal structures for both **1** and **3**, and **2** and **4**.

Solution NMR Spectroscopy. Aluminum(III) Complexes.

The ^{13}C NMR spectrum of **1** in aqueous D_2O solution was taken at pD \sim 8 (Figure 3). Eight main peaks (at 182.4, 179.7, 75.7, 46.2, and 187.5, 179.6, 74.7, 46.0 ppm) were observed vs DSS as an internal standard. Assignment of the observed peaks was aided by the ^{13}C NMR spectrum of citrate, recorded under the same conditions. The peaks corresponding to citrate were observed at 182.4, 179.7, 75.7, and 46.2 ppm. On that basis, the aforementioned eight peaks were attributed to free and Al(III)-bound citrate, respectively (see Table 3). The ^{13}C NMR results listed in Table 3 are similar to those obtained in the past,^{16c} at 4-fold excess of citrate over Al(III), in the pH range 2–8. In those studies, the relatively broad structure of the resonances observed for coordinated citrate had been explained by an equilibrium of coordination isomers. Alternatively, the presence of both mono- and bis-Al(III)–citrate complexes had been evoked as an explanation.

The ^1H NMR spectrum of **1** was taken in D_2O at the same pD value. The spectrum, albeit quite complex, was dominated by two AB quartets (see Figure 2 in Supporting Information). One of those quartets, with sharp resonances at 2.68, 2.64, 2.56, and 2.52 ppm, was attributed to free citrate, while the other one, with significantly broader resonances at 2.67, 2.62, 2.55, and 2.50 ppm, was ascribed to citrate bound in the bis-citrate complex. This behavior does appear to have a precedent, as similar AB quartets were observed for a citrate-titrated aqueous Ga(III) system examined under similar experimental conditions.^{22,36} It should be mentioned here that the chemical shift (δ) and spin–spin coupling (J_{AB}) parameters of the AB spin system of citrate showed changes not only as a function of pH,³⁷ but also as a function of concentration at constant pH. Specifically, we found that in the concentration range 0.02–0.10 M, although J_{AB} remained practically constant, the distance between the two inner lines of the AB quartet increased by about 0.03 ppm, in conjunction with a slight upfield shift (0.003 ppm)

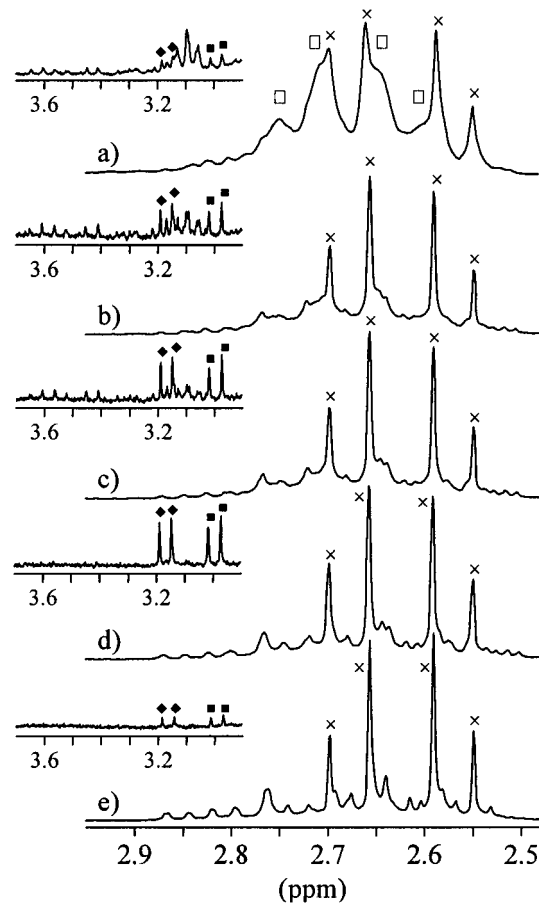


Figure 4. ^1H NMR spectrum of a 0.07 M solution of **3** in D_2O (a) 10 min (pD = 6.32), (b) 25 min, (c) 2 h, (d) 20 h, and (e) 4 days (at thermodynamic equilibrium, pD = 6.06) following dissolution of the complex. Labels: (x), free citrate; (■,◆), citrate complexed in the intermediate 1:1 species; (□), citrate complexed in the 1:2 complex. In all of the spectra, the region between 3.0 and 3.6 ppm is shown as an insert (4-fold spectral enlargement).

Table 4. NMR Spectral Parameters of the Ga(III) Complexes **2** and **4** in the Solid State and in 0.1 M Solutions in D_2O , at $t = 25^\circ\text{C}$. “Bound” Citrate Pertains to the 1:2 Complex

method	complex 2			complex 4			
	solid state	solution (citrate)		solid state	solution (citrate)		
		free	bound		free	bound	
^1H NMR		2.53	2.54		2.55	2.60	
			2.57		2.59	2.64	
			2.63		2.66	2.72	
			2.67		2.70	2.77	
^{13}C NMR	CH ₂	47.3	46.2	46.8	45.5	45.8	
	C	74.2	75.6	74.6	73.6	75.5	
	CO		177.7	179.6	179.7	171.7, 177.5	179.0
			186.6	182.3	187.0	183.4, 188.1	181.8
						178.8	
						185.2	

of the AB quartet’s midpoint. This might be the reason for the small variations in the chemical shifts reported for citrate in the literature.

The observation that (a) the two CH_2COO^- carboxyl and methylene carbons give one signal and (b) the methylene protons give an AB quartet, would suggest a symmetrical coordination of the ligands to Al(III), in solution, via the two terminal carboxylates and the central alkoxy group. This structural formulation is pronouncedly different from that in the solid state, which presents a rather nonsymmetrical arrangement of the

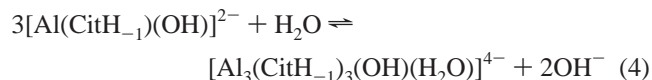
(36) Chang, C. H. F.; Pitner, T. P.; Lenkinski, R. E.; Glickson, J. D. *J. Am. Chem. Soc.* **1977**, *99*, 5858–5863.

(37) Moore, G. J.; Sillerud, L. O. *J. Magn. Reson. (B)* **1994**, *103*, 87–88.

citrate ligands in the coordination sphere of aluminum, with one bound and one free terminal carboxylate (*vide supra*). The fact that, separate signals for the bound and nonbound CH_2COO^- moieties are not observed may also be explained by a fast intramolecular exchange of the two moieties, i.e., the citrate molecules behave fluxionally. This seems to be a more likely explanation than isomerization of the complex upon dissolution. The fact that separate signals are seen for free and bound citrates in solution, however, indicates slow intermolecular exchange of the citrate molecules (see above). The same behavior, observed for a similar Ga(III) –citrate complex,³⁸ was explained by a significantly weaker binding between Ga(III) and the carboxylate groups than the binding to Ga(III) through the central alkoxy oxygen. Accordingly, the alkoxy- O^- acts as an anchor toward the metal ion, while the M(III) –carboxylate bonds are broken and reformed much more rapidly.³⁸ Similar arguments can be invoked in the case of the Al(III) –citrate complexes.

The ^1H NMR spectrum of **1** in D_2O displayed significant changes over time. Specifically, the intensities of free citrate resonances increased, while those of the other AB quartet, belonging to the 1:2 complex, decreased gradually, and finally a rather complicated pattern of signals emerged after about 3 days. In that spectrum (not shown), there exist significant features which include (a) the aforementioned AB quartets for the citrate ligand and (b) characteristic resonances for the asymmetric $[\text{Al}_3(\text{CitH}_{-1})_3(\text{OH})]^{4-}$ trinuclear species^{21b} that appear at 2.86, 2.84, 2.82, 2.80, 2.77, 2.74, and 2.72 ppm.

Taking into account the NMR data for **1**, we suggest the presence of equilibria involving the mononuclear Al(III) –bound citrate(s) as well as the trinuclear Al(III) species. Such a complex set of equilibria emerges upon dissolution of **1** in water, and is shown below (reactions 3 and 4):



The slight increase in the pH of the sample, from pH 7.89 to 8.36, as a function of time, seems to be consistent with the above-proposed overall reaction scheme.

The slow complex formation reactions in the Al(III) –citrate system are fairly well documented in the literature,^{16,39,21b} and explained by the slow oligomerization processes finally yielding the trinuclear species $[\text{Al}_3(\text{CitH}_{-1})_3(\text{OH})]^{4-}$ ($4 < \text{pH} < 8$) and $[\text{Al}_3(\text{CitH}_{-1})_3(\text{OH})_4(\text{H}_2\text{O})]^{7-}$ at $\text{pH} > 9$. The speciation of the complexes formed at the thermodynamic equilibrium state and at a 1:2 metal ion-to-ligand ratio (the same conditions as in the solution of the solid Al(III) –citrate complexes **1** and **3**), reveals that at $\text{pH} \sim 8$, in addition to the asymmetric trinuclear complex $[\text{Al}_3(\text{CitH}_{-1})_3(\text{OH})]^{4-}$, mononuclear 1:2 and 1:1 ternary hydroxo-species coexist in more or less comparable concentrations.

From the dissolution experiment of **1** the identification of Al(III) –citrate mononuclear 1:1 complex is missing. In fact, the concentration of this complex should be the same as that of the free citrate, as both of these species are formed via

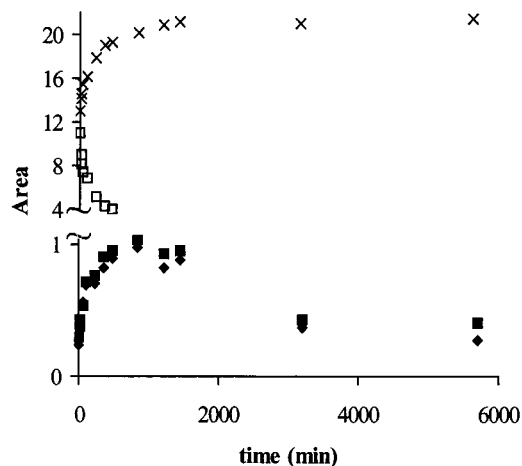


Figure 5. Intensity changes of several selected ^1H NMR signals of **3** in D_2O as a function of time (x) AB quartet of free citrate; (□) signals belonging to the 1:2 complex; (■) and (◆) signals belonging to intermediate 1:1 species (see spectra in Figure 4).

dissociation of the 1:2 complex. A reasonable explanation for that was offered by the detailed study of the dissolution experiment of complex **3**. In this case (Figure 4a), not only the 1:1 complex was missing, but the characteristic broad AB type doublet of the bis-complex did not appear clearly either. To explain this phenomenon, we carried out a kinetic analysis of some well-selected signals. In the region between 2.5 and 3.6 ppm (Figure 4a), three types of signals could be discerned. One type of signals showed a monotonic increase in intensity and was identified as the free citrate. A few other signals decreased with time, i.e., signals in the chemical shift range 3.0–3.2 ppm. Four signals, however, could be clearly identified in this region that first increased in intensity and then decreased over a longer period of time. These results are summarized in Figure 5. It is apparent from the plot that the signal (x) at 2.66 ppm (free citrate) increases at a rate similar to the rate of the decrease of the signal at 2.64 ppm (□). This latter signal may belong to the 1:2 Al(III) –citrate complex. The two doublets, at 3.19, 3.15 ppm (Q, ◆), and 3.01, 2.97 ppm (R, ■), first increase with time, and reach a maximum intensity, but then start to decrease, while the signals belonging to free citrate and the bis-complex do not change over the same period of time. We can tentatively assign Q and R to a 1:1 complex (or complexes), which form(s) the oligomer $[\text{Al}_3(\text{CitH}_{-1})_3(\text{OH})]^{4-}$. Therefore, no free citrate forms and no bis-complex dissociates while the aforementioned species oligomerize(s). Most likely, the 1:1 complexes are not a single species, but rather assemblies of conformers or isomers. They may exist in various forms, producing weak signals unlike those of the free citrate and the bis-complex $[\text{Al}(\text{CitH}_{-1})_2]^{5-}$ at $\text{pH} \sim 8$. This was confirmed by the 2D ^1H -COSY NMR spectrum, taken 26 h following dissolution of complex **3** (see Figure 3 in Supporting Information). There, it is seen that both doublets have their pairs under the strong signals of the trinuclear complex and the free citrate, as the cross-peaks emerge at 2.53, 2.49 ppm, and 2.67, 2.63 ppm, respectively. If one of these doublets is saturated, the intensity of the other one decreases. This suggests that there is an exchange association between them, but that process is slow on the NMR T_2 time scale. Since the bound and unbound CH_2COO^- arms, in the mononuclear complex, should undergo fast intramolecular exchange, these signals probably belong to either two different 1:1 complexes or to a dinuclear complex, which may be the precursor(s) of the trinuclear end product. At higher fields, part of the 2D-

(38) Hawkes, G. E. (private communication) *Texas AMU NMR Newsletter* **1998**, 474–23.

(39) (a) Kiss, T.; Lakatos, A.; Kiss, E.; Martin, R. B. In *Cytotoxic, Mutagenic and Carcinogenic Potential of Heavy Metals Related to Human Environment*; Hadjiliadis, N. D., Ed.; Kluwer Academic Publishers: Netherlands, 1997; pp 241–251. (b) Lakatos, A.; Banyai, I.; Decock, P.; Kiss, T. *Eur. J. Inorg. Chem.* **2001**, 461–469.

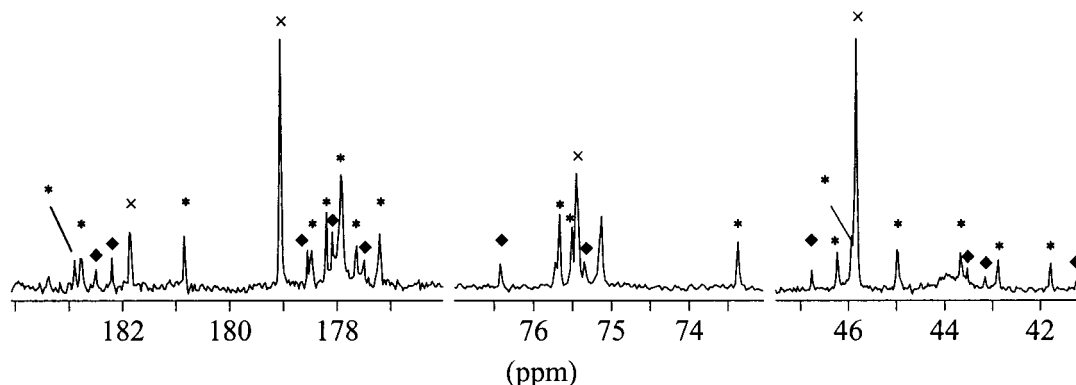


Figure 6. ^{13}C NMR spectrum of a 0.07 M solution of **3** in D_2O taken between 26 and 53 h following dissolution of the complex. Labels: (x) free citrate; (◆) citrate complexed in the 1:1 intermediate species; (*) trinuclear species.

COSY spectrum shows the free citrate doublets and the characteristic 2D spectrum of the $[\text{Al}_3(\text{CitH}_{-1})_3(\text{OH})]^{4-}$ species.⁴⁰

The ^{13}C NMR spectrum of **3** was recorded 26 and 66 h, respectively, following dissolution in water. The 26 h spectrum was very complicated (Figure 6). In addition to the signals of the free citrate (x) and the trinuclear complex (*), the signals of four extra CH_2 carbons, four central carbons, and seven or eight terminal COO^- carbons (◆) could be recognized, indicating the presence of intermediate species. In the latter spectrum (66 h), close to the equilibrium-state, only the free citrate and the trinuclear species were present, aside from traces of the bis-complex.

The ^{27}Al NMR spectrum of **1** was also recorded in H_2O . The spectrum of **1** in equilibrium solutions, showed a broad ($w_{1/2} = 560$ Hz) asymmetric signal with a maximum at 11.84 ppm (vs AlCl_3) and a shoulder at a higher field. Moreover, experiments carried out in the $\text{Al}(\text{III})$ –citrate (1:1) system, by mixing $\text{Al}(\text{III})$ and citrate in 1:1 molar ratio, and adjusting the pH to neutral, revealed relatively limited changes in the ^{27}Al NMR spectra of the major component over time.^{39b} The spectral pattern of the equilibrium sample, measured on a 130.29 MHz instrument, agreed with the one described in the literature^{21b} for the trinuclear complex. The above results suggest that, under the prevailing experimental conditions, no significant alteration was involved in the coordination number and/or geometry of the predominant complex(es), and the trinuclear complex $[\text{Al}_3(\text{H}_{-1}\text{Cit})_3(\text{OH})]^{4-}$ was the predominant $\text{Al}(\text{III})$ species in equilibrium solutions, at neutral pH, either at the 1:1 or 1:2 metal-to-ligand ratio.

Gallium(III) Complexes. The ^{13}C NMR spectra of **2** and **4** were measured at the autogenous pH, upon dissolution in D_2O . The spectra, in many respects, resembled those of the corresponding $\text{Al}(\text{III})$ complexes (Figure 3): the observed two sets of resonances were attributed to the free citrate and bound citrate in the 1:2 complex. The results are in good agreement with those obtained by Chang et al. (see Figure 2a–c in ref 36). As in the case of the $\text{Al}(\text{III})$ –citrate complex, here as well, no clear ^{13}C NMR resonances could be detected for the 1:1 complex, which should be formed via dissociation of the 1:2 complex. An analogous observation was made by Hawkes.³⁸

The ^1H NMR spectra of complexes **2** and **4** consisted of two AB quartets (Table 4) and numerous minor resonances in the δ range of 2.5–3.6 (Figure 7). The intensities of these “extra” peaks and those of the peaks in one of the AB quartets (x), decreased significantly at high concentrations of the complexes. This suggests that the AB quartet (□) can be assigned to the 1:2 complex, while the “extra” peaks belong to some form of

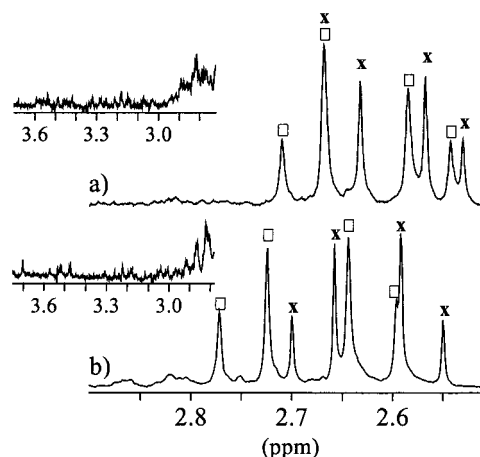


Figure 7. ^1H NMR spectrum of 0.1 M of the $\text{Ga}(\text{III})$ complexes in D_2O (a) **2**, $\text{pD} = 7.7$, (b) **4**, $\text{pD} = 6.0$. Labels: (x) free citrate; (□) citrate complexed in the 1:2 species. In both a and b spectra, the region 2.8–3.6 ppm is shown as an insert (3-fold spectral enlargement).

1:1 species, presumably representing oligonuclear as well as mononuclear entities. The correct assignment of the two AB quartets was confirmed by adding an extra amount of citrate to the sample, thereby shifting the equilibrium:



to the left (because of the possibility of the formation of 1:1 oligonuclear complexes, this equilibrium may imply a cascade of consecutive equilibria between various 1:1 species). Hawkes³⁸ has suggested that of the two ^1H NMR AB quartets, the one at higher field belongs to free citrate, while the other one is a composite of signals belonging to both 1:2 and 1:1 complexes. On the basis of the average line width for the four lines of the two AB patterns, it was found that the lines belonging to bound citrate were $0.35 (\pm 0.30)$ Hz broader than the average line width of the lines of free citrate. We do not think that this minute broadening is sufficient to suggest a superposition of the signals of both the 1:1 and 1:2 species in the AB quartet (□). We would like to point out, however, that at lower temperature, the lines of the coordinated citrate broaden significantly, indicating that an exchange process might be in place. It is not unreasonable to postulate that this exchange process involves an intramolecular (resulting in fluxionality) rather than intermolecular fast exchange of citrate between the 1:1 and 1:2 complexes.

Unfortunately, no systematic solution speciation study has been carried out so far on the $\text{Ga}(\text{III})$ –citric acid system that will allow calculation of species distribution for the experimental

conditions of our NMR measurements. Harris and Martell,⁴¹ and Skorik and Artish⁴² carried out potentiometric titrations only in equimolar solutions, and determined stability constants only for the mononuclear complexes $[\text{Ga}(\text{cit})]$ and $[\text{Ga}(\text{CitH}_{-1})]^{-}$. At the same time, Chang et al.³⁶ estimated stepwise conditional stability constants for 1:1 and 1:2 Ga(III)–citrate complexes at $\text{pD} \sim 5.4$ ($K_1 = 48 \text{ M}^{-1}$, $K_2 = 18 \text{ M}^{-1}$). Using these equilibrium constants, the percentage fractions of the various Ga(III)–citrate species and free citrate, being at equilibrium in solution, were calculated. For a total concentration of $c_{\text{Ga(III)}} = 0.07 \text{ M}$ and $c_{\text{citrate}} = 0.14 \text{ M}$, the fraction of citrate bound in the 1:2 complex, the fraction of citrate bound in the 1:1 complex, and the fraction of free citrate were found to be 0.36, 0.24, and 0.40, respectively. The integration of the deconvoluted major peaks (the two AB quartets) of the ^1H NMR spectrum of complex **4**, at $\text{pD} 6.0$, gave fractions of 0.55 for the 1:2 complex, and 0.45 for the free citrate. No accurate deconvolution could be carried out for all species, especially for the 1:1 complex(es). The aforementioned determination of percentage fractions suffers from high uncertainty, because part of the 1:1 host signals may lie beneath the more intense resonances of the 1:2 complex and the free citrate. Furthermore, an integration of that part of “minor signals”, which are not buried under the intense resonances accounted for about 70% of the free citrate signals. Considering the uncertainty, and the possibility that a few other “minor signals” were left out of the integration, it is not unreasonable to envisage that the “missing” intensity of the 1:1 complex is there. Very likely, that “missing” intensity may not correspond to a single complex, but a mixture of 1:1 monomeric and oligomeric binary and ternary hydroxo species. To that end, offered as a further proof, a 0.1 M 1:1 Ga(III)–citrate solution was prepared at $\text{pH} \sim 4$, and the ^1H NMR spectrum was recorded. A similar, not well-resolved, assembly of peaks was recorded as the “minor signals” in our samples. To diminish this source of uncertainty in peak integration, the ratio of citrate bound in the 1:2 complex to free citrate was calculated to be 0.47:0.53, fairly close to the ratio 0.55:0.45 indicated by the ^1H NMR data. As a final proof of the ^1H NMR line assignment, when the pH of the solution of compound **4** was adjusted to 4.5 (the optimal pH for the formation of 1:1 oligonuclear Ga(III)–citrate complexes^{11d,36}), the intensity of the “extra” signals increased considerably, in addition to some broadening and upfield shift of the main signals assigned to mononuclear complexes. These results confirmed the assertion that the “extra” lines belong to 1:1 oligonuclear species. On the basis of the line broadening of the citrate ^1H NMR resonances and dialysis experiments, Glickson et al.^{11d} suggested the formation of oligomeric complexes in the pH range 3–7. Further, Harris and Martell⁴¹ proposed an overall stoichiometry of $[\text{Ga}_3(\text{H}_{-1}\text{Cit})_3(\text{OH})]^{4-}$ for the oligomeric species (the same composition as in the case of the Al(III)-oligomer).^{21b} Due to the large number of signals and their occurrence in a very wide field range, the presence of more than one species could be suggested in an equilibrium encompassing mononuclear as well as oligonuclear 1:1 complexes. Interestingly enough, the NMR spectra of the Ga(III) complexes showed no time dependence, indicating significantly faster solution equilibration than in the case of the corresponding Al(III) complexes.

Discussion

Stoichiometric reactions between the metal ion M(III) ($\text{M} = \text{Al}, \text{Ga}$) and citrate were carried out in water and led to

crystalline complexes **1–6**. The pH of the aqueous solution played a key role in the syntheses of those complexes. Thus, pH -dependent reactions yielded mononuclear octahedral assemblies comprised of M(III) (Al, Ga) and citrate in a 1:2 stoichiometry, with the two coordinated citrate ligands being identical or distinctly different in their protonation state. Metal-to-citrate ratios other than 1:2 (e.g., 1:1) were also employed, yet the only species isolated, albeit in lower yield, were those bearing the 1:2 metal to citrate stoichiometry. In **1** and **2**, the presence of different metal ions, Al(III) and Ga(III), did not result in any significant differences between their coordination geometries. This assertion was confirmed by the similarity of the solid state ^{13}C -MAS NMR spectra in **1** and **2**: two different CH_2 carbons of the bound and unbound carboxylates strongly overlapping, two identical central carbons and two identical central carbonyl carbons at lower field, and two different terminal carbonyl carbons of the bound and unbound carboxylates strongly overlapping could be observed for both the Al(III) and Ga(III) complexes. Waters of crystallization were present in the lattice, assisting in the formation of a hydrogen-bonding network conferring stability upon the lattice. Such a contention could (at least) partly be reflected in the exceptional stability of the crystalline materials over long periods of time.

In complexes **3–6**, bearing a 4– charge, one of the bound citrates was fully deprotonated, while the other one was triply deprotonated carrying a hydrogen on the pendant carboxylate group. This led to broadening of the overlapping signals of the four CH_2 carbons in the MAS ^{13}C NMR. As a consequence, only the two bound terminal carboxylate carbons were identical, with the unbound carboxylate carbons being different (protonated or deprotonated carboxylates), resulting in a partial separation of the observed signals. Hence, protonation of one of the CH_2COO^- moieties led to a ~ 5 ppm upfield shift of one of the carbonyl signals. A similar splitting was observed in the signals of the central carboxylate carbonyls (see Figure 2). The significance of that protonation is high, as the hydrogen in question seeks to form a hydrogen bond with the other pendant terminal carboxylate group of the adjacent metal-citrate assembly in the lattice. Consequently, a one-dimensional array of metal–citrate complexes forms in the lattice that is held together by hydrogen bonds. Beyond the hitherto accounted for differences and similarities, there also exist profound conformational changes associated with the bound citrates on both the 5– and 4– complexes (not shown). Such changes could be one of the reasons for the splitting of the carboxylate carbonyl resonances observed in the ^{13}C -MAS spectra of **3**.

It is worth noting that under the experimental conditions reported in this work, the well-known trinuclear complex, which was characterized by X-ray crystallography in the solid state,^{21b} and by NMR in solution,^{21b,40} could not be isolated. It appears, therefore, that in a pH -variable speciation pattern of M(III) (Al, Ga) with citrate in a 1:2 ratio, both classes of species (**1,2/3,4**) exist and can interconvert as a function of pH . This is an interesting feature of the title complexes, as it is known from solution speciation studies in the Al(III)–citrate system^{16,17} and the less clarified Ga(III)–citrate system,^{38,41} that the 1:2 complexes, isolated here, exist as the predominant species only at a fairly high excess of citrate, while at comparable metal-to-ligand ratios, 1:1 oligonuclear complexes are the major species.

The behavior of the solid complexes upon dissolution (reactions 3 and 4) was followed by multinuclear NMR techniques. The results showed that Al(III) and corresponding Ga(III)–citrate complexes exhibited very similar transformations

(40) Bodor, A.; Banyai, I.; Zekany, L.; Toth, I., to be submitted.

(41) Harris, W. R.; Martell, A. E. *Inorg. Chem.* **1976**, *15*, 713–720.

(42) Skorik, N. A.; Artish, A. *Sz. Zh. Neorg. Khim.* **1985**, *30*, 1994–1997.

upon dissolution in water and supported strongly the formation of intermediate dinuclear complexes with rather unsymmetrical geometries. There was, however, a significant difference in the time scale of the reactions. Specifically, the Ga(III) complexes showed much faster equilibration times than the corresponding Al(III) complexes, as that was indicated by the unchanged NMR spectra of the former complexes as a function of time. Taking into account that the rate of exchange reactions for Ga(III) is generally about 1000 times faster than that for Al(III),⁴³ the observation that all equilibria, including oligomerization processes, were reached in less than 10–20 min (the minimum time elapsed between sample preparation and recording of the first NMR spectrum) in the Ga(III) case, was in accordance with expectations.

Overall, the data presented in this work confirm the presence of low MW, mononuclear aluminum and gallium–citrate complexes in aqueous solutions of different pH. The pH dependence of their structural and spectroscopic properties jibes well with results from past solution studies of such systems and enhances their status as potential components in speciation patterns relevant to biological media. The chemistry of citrate with Al(III) and Ga(III) in aqueous solutions has proven that citrate can promote solubilization of those metal ions in the physiological pH range, thus offering plausible explanations for citrate's contribution to the accumulation of aluminum and gallium in biological tissues and any further influence on their

bioavailability. Thus, for issues ranging from the biotoxicity of aluminum (possible association with Alzheimer's disease) to the selective accumulation of gallium in specific tissues for subsequent imaging and treatment, the complexes presented here provide valuable information for further perusal. To that end, structurally diverse, low MW species, mononuclear or oligonuclear, preferably with lower anionic or zero charge for efficient permeation of the blood brain barrier, are currently being investigated in our labs.

Acknowledgment. This work was carried out in the framework of a COST D8 collaboration and was supported with funds provided by the Department of Chemistry, University of Crete, Greece, and the Ministry of Culture and Education, Hungary (FKFP 0013/97 and OTKA 23776/97). We thank NATO for a Collaborative Research Grant (CRG 971566) and GSRT for a grant (7638/924-5-99) to A.S. The financial assistance to Drs. C.P.R. and A.T. by the Agricultural Bank of Greece (A.T.E.) and Mr. John Boutaris is gratefully acknowledged.

Supporting Information Available: Tables of X-ray crystal data, positional and thermal parameters for $(\text{NH}_4)_5[\text{M}(\text{C}_6\text{H}_4\text{O}_7)_2] \cdot 2\text{H}_2\text{O}$ ($\text{M} = \text{Al}^{3+}$ (**1**), Ga^{3+} (**2**)), $(\text{Cat})_4[\text{Al}(\text{C}_6\text{H}_4\text{O}_7)(\text{C}_6\text{H}_5\text{O}_7)] \cdot n\text{H}_2\text{O}$ [$\text{Cat} = \text{NH}_4^+$, $n = 3$ (**3**); $\text{Cat} = \text{K}^+$, $n = 4$ (**5**)] and $(\text{Cat})_4[\text{Ga}(\text{C}_6\text{H}_4\text{O}_7)(\text{C}_6\text{H}_5\text{O}_7)] \cdot n\text{H}_2\text{O}$ [$\text{Cat} = \text{NH}_4^+$, $n = 3$ (**4**); $\text{Cat} = \text{K}^+$, $n = 4$ (**6**)]. An ORTEP Figure of complex **2**, Figures for the ^1H NMR spectrum of complex **1** in D_2O , 2D ^1H -COSY NMR spectrum of complex **3** in D_2O , and ^{13}C NMR spectrum of complex **2** in D_2O . This material is available free of charge via the Internet at <http://pubs.acs.org>.

(43) Hugi-Cleary, D.; Helm, L.; Merbach, A. *J. Am. Chem. Soc.* **1987**, *109*, 4444–4450.